Th SRS1 14

Generalizing and Stabilizing Reverse Time Migration Deconvolution Imaging

J. Messud* (CGG) & G. Lambaré (CGG)

SUMMARY

For reverse time migration, the deconvolution imaging condition offers the strongest possibility for source designature and compensation of illumination, but cross-correlation-based imaging conditions are currently the most widely used due to their high stability. We propose here a general theoretical frame and practical solution for stabilizing deconvolution-based reverse time migration. Our approach involves an optimization scheme regularized by a set of constraints. The proposed constraints insure both high resolution and removal of low frequency migration noise arising in the case of diving or reflected waves in the background model. We show the improvement obtained with our approach on synthetic and real datasets.

Introduction

Reverse Time Migration (RTM) has become a commonly-used high-quality tool to image complex media (Zhang and Sun, 2009). While always based on numerical solutions of the wave equation the various RTM kernels may differ by their imaging principle. The most commonly used are the cross-correlation-based ones favored by their unconditional stability (Claerbout, 1971). however, these require pre/post-processing for source wavelet removal, and are hardly "true amplitude" (Zhang and Sun, 2009). The deconvolution imaging condition (Claerbout, 1971), which naturally provides a better source wavelet removal, also potentially improves illumination compensation (and thus amplitude preservation (Keho and Beydoun, 1988)), and reduces migration cross-talk due to multiples and multi-pathing (Poole et al., 2010; Whitmore et al., 2010). For these reasons, deconvolution would be preferred in the presence of complex velocity models and/or multiples if not for the serious instabilities and artefacts resulting from its use (Guitton et al., 2007, Claerbout, 1971).
Here, we revisit RTM with a new deconvolution-based imaging principle. We propose a general formalism based on optimization theory, mitigating the pitfalls of deconvolution imaging while enhancing its resolution (through a sparseness constraint) and attenuating artefacts such as the low frequency migration noise that arise in the case of diving waves or back scattering by sharp velocity contrasts (Zhang and Sun, 2009, Yoon and Marfurt, 2006) (Figure 1).

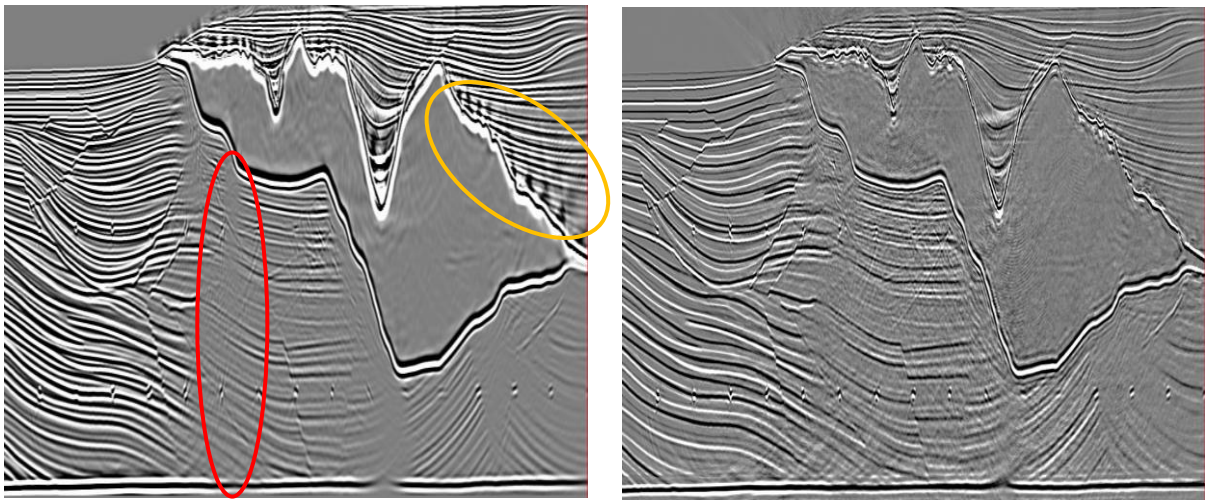

Figure 1 Sigsbee2a data. *Left: A typical cross-correlation RTM stack image. It exhibits illumination issues (red ellipse) and back scattering noise (yellow ellipse) which has been partly attenuated by a post-migration Laplacian filter (Zhang and Sun, 2009). Right: Proposed new imaging condition stack.*

Deconvolution imaging condition

In his pioneering paper, Claerbout (1971) established depth migration through an imaging principle where the subsurface image is built taking the zero time cross-correlation of the incident and reflected wave fields at the image point:

$$I_{cor}(\boldsymbol{x},\boldsymbol{s}) = \left[P_{ref} \times P_{inc}\right](\boldsymbol{x},\boldsymbol{s},t=0) = \int d\omega \left[P_{ref}{}^{*} P_{inc}\right](\boldsymbol{x},\boldsymbol{s},\omega) \quad . \tag{1}$$

$P_{inc}(\boldsymbol{x},\boldsymbol{s},t)$ denotes the incident wave field at position $\boldsymbol{x}$ in the image for a source position $\boldsymbol{s}$ and a time t (corresponding angular frequency is ω), $P_{ref}(\boldsymbol{x},\boldsymbol{s},t)$ denotes the reflected wave field, × denotes time correlation and * denotes complex conjugation. Claerbout (1971) also emphasized that when using a deconvolution imaging principle, $I_{dec}(\boldsymbol{x},\boldsymbol{s}) = \int d\omega \left[P_{ref} / P_{inc}\right](\boldsymbol{x},\boldsymbol{s},\omega)$, the image is (under some assumptions) a reflectivity function directly proportional to the local reflection coefficient, $\mathcal{R}(\boldsymbol{x},\boldsymbol{s})$,

$$I_{dec}(\boldsymbol{x},\boldsymbol{s}) = \int_{-\omega_{max}}^{\omega_{max}} d\omega \left[P_{ref} / P_{inc}\right](\boldsymbol{x},\boldsymbol{s},\omega) \approx 2\omega_{max}\mathcal{R}(\boldsymbol{x},\boldsymbol{s}) \quad . \tag{2}$$

This interpretation relies on assumptions of Kirchhoff forward modelling and migration, i.e. high frequency asymptotic approximation, linearization, pre-critical reflection, full illumination and a single wave path from source point to any image point (Stolk and Symes, 2004, Bleistein et al., 2001). Thus the deconvolution imaging condition preserves amplitude. Moreover it is potentially more accurate than the classical cross-correlation imaging condition even if it suffers from instabilities and

artefacts which are difficult to mitigate (Guitton et al., 2007). We develop a practical formalism and implementation for stabilizing and improving deconvolution RTM.

Deconvolution RTM as an optimization problem

The idea is to set deconvolution migration as a constrained optimized problem, i.e. finding the distribution of reflection coefficients, $\mathcal{R}(\mathbf{x},\mathbf{s},\omega)$ (in its general form we allow it to depend on ω), such that the following cost function is minimal. We denote $\|a(\mathbf{x},\mathbf{s},\omega)\|^p = \int d\,\mathbf{x}d\,\mathbf{s}\,d\omega|a(\mathbf{x},\mathbf{s},\omega)|^p$:

$$C[\mathcal{R}] = \frac{1}{2}\left\|\beta(\mathbf{x},\mathbf{s},\omega)\left[P_{ref}\,/\,P_{inc}\right](\mathbf{x},\mathbf{s},\omega) - \mathcal{R}(\mathbf{x},\mathbf{s},\omega)\right\|^2 + constr\left[\mathcal{R}(\mathbf{x},\mathbf{s},\omega)\right]. \quad (3)$$

$\beta(\mathbf{x},\mathbf{s},\omega)$ is a "data" weight compatible with preserved-amplitude migration and $constr[\mathcal{R}(\mathbf{x},\mathbf{s},\omega)]$ is any set of appropriate constraints on the reflectivity. $\beta(\mathbf{x},\mathbf{s},\omega)$ should vary smoothly in the ω -direction and insure no singularity due to very small values of $P_{inc}(\mathbf{x},\mathbf{s},\omega)$, for example

$$\beta = P_{inc}^{*}P_{inc}\,/\left\langle\left|P_{inc}\right|^2\right\rangle_{regul}, \quad (4)$$

where the regularized $<|P_{inc}|^2>_{regul}$ can be obtained using smoothing and damping (Guitton et al., 2007). The constraints on $\mathcal{R}(\mathbf{x},\mathbf{s},\omega)$ should at least force it to be non-oscillating in the ω-direction, but can also contain any other physical constraint.

The principle behind eq. (3) is that, within assumptions of Kirchhoff forward modelling and migration, we can recover the reflectivity by "cleaning" P_{ref}/P_{inc} of its ω-direction "oscillatory" components (explaining the choice of an L_2-norm optimization on the data). This is in agreement with the principle of Claerbout (1971) that can be reformulated: Reflectors exist at points in the ground where the incident wavefield finds frequency coherence with the reflected wavefield.

Within the high-frequency hypothesis $\mathcal{R}(\mathbf{x},\mathbf{s},\omega)$ does not depend on ω; we then have $\mathcal{R}(\mathbf{x},\mathbf{s})$. This represents the conventional reflectivity function that is the basis for amplitude versus angle (AVA) studies and recoverable through true or preserved amplitude migration (Bleistein et al., 2001). We will stick to this approximation from now on.

This formalism provides (up to a multiplicative constant) Claerbout's regularized deconvolution imaging condition (Claerbout, 1971, Guitton et al., 2007) when $\beta(\mathbf{x},\mathbf{s},\omega)$ is limited to eq. (4) and no constraint is introduced. In its general form, eq. (3) generalizes the deconvolution imaging condition, allowing various types of physical or geological constraints.

Constraints for high resolution and low frequency noise removal

As a constraint on the reflectivity we propose an L_p-norm constraint,

$$constr\left[\mathcal{R}(\mathbf{x},\mathbf{s})\right] = \left\|\gamma(\mathbf{x},\mathbf{s})\mathcal{R}(\mathbf{x},\mathbf{s})\right\|^p\,/\,p, \quad (5)$$

where $\gamma(\mathbf{x},\mathbf{s})$ is a weighting factor and $p<2$ is real and positive. If the true reflectivity of the subsurface can be represented as a sparse spike series, an L_1-norm constraint (i.e. $p=1$) will recover the spike train (Taylor et al., 1979), hence the name "high resolution" constraint. Indeed an L_1-norm penalizes less the strong or isolated reflectors in $\mathcal{R}(\mathbf{x},\mathbf{s})$ than a L_2-norm, thus allowing the isolation and spiking of those reflectors. If the spike train assumption is too strong according to true subsurface properties, we propose to increase p (keeping it <2), relaxing this assumption. The optimum p value thus depends on the subsurface. $\gamma(\mathbf{x},\mathbf{s})$ must be tuned according to uncertainties in $\mathcal{R}(\mathbf{x},\mathbf{s})$ to favor high-resolution without generating noticeable artifacts.

A second issue that can naturally be solved within the frame of our formalism is the removal of low frequency migration noise. This appears when incident and reflected waves propagate locally along nearly parallel directions, i.e. for diving waves or in case of reflected events due to a sharp contrast in the propagating velocity (for instance due to salt) (Zhang and Sun, 2009), in violation of migration theory assumptions. Several solutions have been proposed for remedying this. Among them we have the application of a Laplacian filter to the image as a post-processing (Zhang and Sun, 2009), or the elimination of the components of the data producing the artefact in the propagated wave fields using, for example, Poynting vectors (Yoon and Marfurt, 2006). Note that this can be accounted for within our formalism by adding a propagation direction to $\beta(\mathbf{x},\mathbf{s},\omega)$. While these approaches can be efficient they also have drawbacks in terms of accuracy or computing efficiency (Guitton et al., 2007b).

Low frequency migration noise is caused by effects that violate Kirchhoff modelling and migration assumptions. We propose to parameterize their contribution to the "non-oscillatory" part of P_{ref}/P_{inc}, by including in expression (3) a decomposition of the migrated image into a reflectivity part, $\mathcal{R}(\mathbf{x},\mathbf{s})$, and a noise part, $S(\mathbf{x},\mathbf{s})$,

$$C[\mathcal{R},S]=\frac{1}{2}\left\|\beta(\mathbf{x},\mathbf{s},\omega)\left([P_{ref}\ /\ P_{inc}](\mathbf{x},\mathbf{s},\omega)-\mathcal{R}(\mathbf{x},\mathbf{s})-S(\mathbf{x},\mathbf{s})\right)\right\|^2+constr[\mathcal{R}(\mathbf{x},\mathbf{s}),S(\mathbf{x},\mathbf{s})]. \quad (6)$$

Considering $S(\mathbf{x},\mathbf{s})$ as low frequency noise, we choose a constraint

$$constr[\mathcal{R}(\mathbf{x},\mathbf{s}),S(\mathbf{x},\mathbf{s})]=\left\|\gamma(\mathbf{x},\mathbf{s})\mathcal{R}(\mathbf{x},\mathbf{s})\right\|^p\ /\ p+smooth[S(\mathbf{x},\mathbf{s})], \quad (7)$$

where $smooth[S(\mathbf{x},\mathbf{s})]$ denotes a smoothness constraint (in the $\mathbf{x}$-domain) on S, that can be implemented using a second-order spatial derivative. Eq. (6) is resolved by a joint iterative non-linear inversion of $\mathcal{R}$ and S. It allows the "cleansing" of the reflectivity from S in each of the common shot migrated gathers. If $\beta(\mathbf{x},\mathbf{s},\omega)$ is chosen as in eq. (4), eq. (6) can be reformulated as a post-processing of common shot gather migrated using regularized deconvolution.
The approach of removing low frequency migration noise by minimizing a least squares cost function has been used by Guitton et al. (2007b). Here we use different constraints and a general formalism.

Applications

We present the application of our new approach (eq. (6)) involving deconvolution with a high resolution constraint and low frequency noise removal to a synthetic and a real dataset. We compare the results obtained with our approach to those obtained with a more conventional RTM involving a cross-correlation imaging condition, amplitude compensation and Laplacian post-processing for low frequency noise removal (Zhang et al., 2009).
Figures 1 to 3 show results on the synthetic Sigsbee dataset (Guitton et al., 2007). Figure 1 shows an overall view, and underlines that illumination is increased under the salt and amplitudes are better balanced with the new imaging condition because it is deconvolution-based. Figure 2 shows the ability of the new imaging condition to remove the low frequency migration noise due to the strong reflections at the base and top of salt. Note that the result obtained with the cross-correlation RTM and the Laplacian filter have also significantly attenuated the artefact. Figure 3 shows that the new imaging condition has the ability to increase resolution in zones where there is no salt, compared to both cross-correlation and unconstrained deconvolution.
Figures 4 shows the results on a real dataset. The source wavelet was estimated with a standard process and we can observe the improved resolution obtained with our new imaging condition.

Conclusion

Conventional deconvolution based RTM suffers from stabilization issues, and we have developed a general frame for its regularization. The problem is set as an optimization problem for which we have the possibility to introduce various types of constraints. We have presented two types, one for enhancing resolution under the hypothesis of reflector sparseness and a second for removing low frequency migration noise. Applications on the Sigsbee synthetic and on a real dataset show the improvements brought by the approach compared to a conventional cross-correlation based RTM.

Acknowledgements

We thank CGG for the permission to publish this work, and GDF Suez E&P Nederland B.V. for the permission to show the seismic data. We thank Botao Qin and Ghislain Viguier for their involvement on various aspects of the subject.

References

Bleistein, N., Cohen, J.K., Stockwell, J.W. [2001] *Mathematics of Multidimensional Seismic Imaging, Migration, and Inversion*. Springer-Verlag, New-York.
Claerbout, J. [1971] Toward a unified theory of reflector mapping. *Geophysics*, **36**, 467.
Guitton, A., Valenciano, A., Bevc, D., Claerbout, J. [2007] Smoothing imaging condition for shot-profile migration. *Geophysics*, **72**, S149.
Guitton, A., Kaelin, B., Biondi, B. [2007b] Least-squares attenuation of reverse-time-migration artifacts. *Geophysics*, **72**, S19.

- Keho, T.H., Beydoun, W.B., 1988. Paraxial ray Kirchhoff migration, Geophysics, 53, 12, p. 1540-1546.
- Lu, S., Whitmore, N.D., Valenciano, A.A., Chemingui, N., 2011. Imaging of primaries and multiples with 3D SEAN synthetic, SEG San Antonio Annual Meeting.
- Poole, T.L., Curtis, A., Robertsson, J.O.A., Van Manen, D.J., 2010. Deconvolution imaging conditions and cross-talk suppression, Geophysics, Vol. 75, W1.
- Stolk, C.C., Symes, W.W., 2004. Kinematic artifacts in prestack depth migration, Geophysics, 69, 2, p. 562–575.
- Taylor, H.L., Banks, S.C., McCoy, J.F., 1979. Deconvolution with the L_1, norm, Geophysics, 44, 1, p. 39-52.
- Whitmore, N.D., Valenciano, A.A., Solner, W., 2010. Imaging of primaries and multiples using a dual-sensor streamer, SEG Denver Annual Meeting.
- Yoon, K., Marfurt, K.J., 2006. Reverse-time migration using the Poynting vector, Exploration Geophysics, Vol. 37, p. 102-106.
- Zhang, Y., Sun, J., 2009. Practical issues of reverse time migration: true-amplitude gathers, noise removal and harmonic-source encoding, First Break, Vol. 26, p. 19-25.

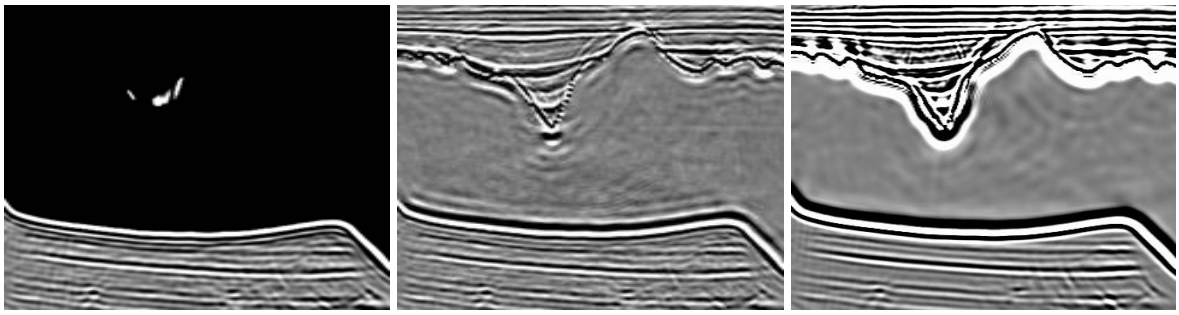

Figure 2 Sigsbee2a data, top and base of salt. *Left: Unconstrained deconvolution (low frequency migration noise above base of salt). Middle: New imaging condition. Right: Cross-correlation (with Laplacian filtering).*

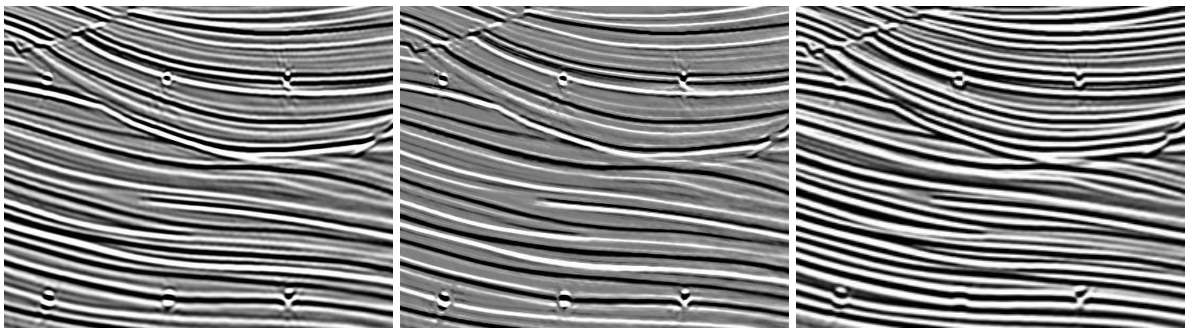

Figure 3 Sigsbee2a data, sediment area. *Left: Unconstrained deconvolution. Middle: New imaging condition. Right: Cross-correlation.*

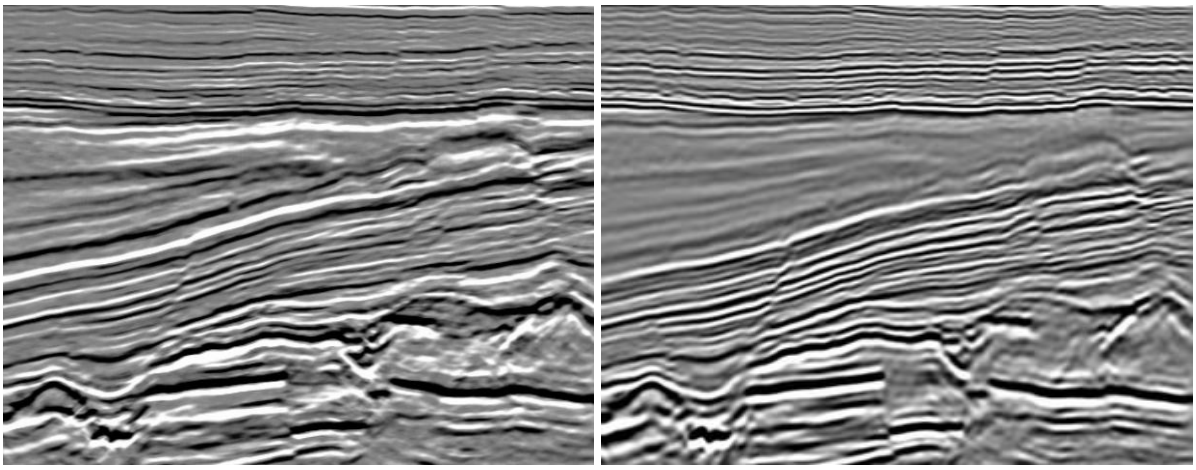

Figure 4 Real data. *Left: New imaging condition. Right: Cross-correlation.*